Microscopic order parameters in PrAlO$_3$

M. D. Sturge,* E. Cohen,† and L. G. Van Uitert

Bell Laboratories, Murray Hill, New Jersey 07974

R. P. van Stapele

Philips Research Laboratories, Eindhoven, The Netherlands

(Received 19 February 1975)

The electron spin resonance of Gd^{3+} impurities in single crystals of PrAlO$_3$ has been studied in the temperature range 4.2 to 295 K. The fine structure can be explained in terms of a spin Hamiltonian whose largest term is an almost axial second-rank tensor, which is closely related to the local distortion at the rare-earth site. The direction of the principal axis of this tensor shifts discontinuously from [111] to [10$\bar{1}$] at the 205-K trigonal-orthorhombic phase transition. Below the 151-K second-order phase transition, the angle between the principal axis and [10$\bar{1}$] varies continuously with temperature. Below 70 K the principal axis lies within 1° of [001], and the symmetry is almost exactly tetragonal. From the direction of the principal axis we derive an order parameter describing local ("internal") displacements. We also measured the splitting and symmetry of the lowest electronic states of PrAlO$_3$ by optical absorption. Our results are more accurate than previous fluorescence measurements. From this splitting, an "electronic" order parameter can be derived. We find that for $T > 0.8 T_c$ these two order parameters are equal to each other and to a third, the reduced macroscopic strain, which has been measured previously by Birgeneau *et al*. This agreement is predicted by Feder and Pytte's theory of cooperative Jahn-Teller phase transitions. The order parameters are found to follow the classical $(T_c - T)^{1/2}$ behavior to within 0.2° of T_c. At 118 K (0.785T_c), where a pronounced acoustic anomaly has been reported by Fleury *et al*., we find only a very weak anomaly in the temperature dependence of the internal-displacement order parameter, and no detectable effect on that of the other two parameters.

I. INTRODUCTION

Recently there have been several important advances in the understanding of the phase transitions of PrAlO$_3$. This crystal undergoes a succession of phase transitions from the cubic perovskite structure, through trigonal, orthorhombic, monoclinic to an essentially tetragonal structure at $T = 0$.[4,2] Harley *et al*.[3] have proposed a model which describes the various distortions from cubic symmetry in terms of rotations of the AlO$_6$ octahedra which are coupled to the electronic $^3H_4$ levels of the Pr^{3+} ions through the electron-phonon interaction. Birgeneau *et al*.[4] studied the 151-K second-order phase transition between the orthorhombic and monoclinic phases and showed that it was driven by the coupling of the lowest-lying exciton to the phonons. It is thus well established that PrAlO$_3$ exhibits both a first-order transition (trigonal-orthorhombic at 205 K) and a second-order transition, which are both due to the electron-phonon interaction.

The dynamics of such transitions (usually referred to as cooperative Jahn-Teller transitions) have been discussed theoretically by Feder and Pytte.[5] They have studied a simplified model of an ionic system with doubly degenerate electronic levels coupled to both the optical phonons and elastic strains. For such a system, order parameters can be derived from the splitting of the electronic

levels, the macroscopic strain, and the appropriate internal displacements, and each order parameter is expected to show the same temperature dependence close to the transition temperature. While PrAlO$_3$ is somewhat more complex than this model, it is probably a unique system, in that each of these three order parameters can be measured independently: the electronic splitting by optical absorption,[1] fluorescence,[3] and electronic Raman effect[3,6,7]; the macroscopic strain by elastic neutron scattering,[4] and the internal displacements by electron spin resonance.[8]

The model of Harley *et al*.,[3] as refined in the light of subsequent work, is as follows. It is an extension of the well-known model of structural phase transitions in LaAlO$_3$ and SrTiO$_3$, which are isomorphous with PrAlO$_3$ in the high-temperature (cubic perovskite) phase. The structure of this phase is illustrated schematically in Fig. 1. In LaAlO$_3$ at 760 K, as in PrAlO$_3$ at 1320 K, there is a second-order transition from cubic to trigonal symmetry.[9] The distortion consists of a staggered rotation of AlO$_6$ octahedra about a ⟨111⟩ axis. Similarly, SrTiO$_3$ at 105 K undergoes a transition to a tetragonal phase in which the staggered rotation is about a ⟨001⟩ axis.[10] These spontaneous rotations are due to anharmonic interatomic forces and are the subject of several illuminating review papers.[9,11] In PrAlO$_3$ as in LaAlO$_3$, these forces favor a trigonal distortion. However, Pr^{3+} differs from La^{3+}
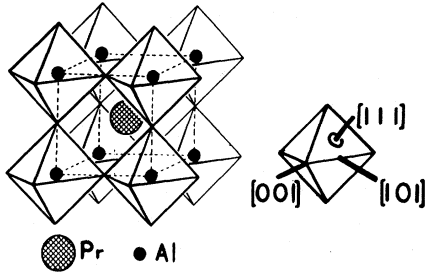
FIG. 1. Perovskite structure, showing how the AlO_6 octahedra form a cube around the Pr^{3+} ion. There is an O^{2-} ion at each corner of each octahedron, shared between adjacent octahedra. In the distorted phases the octahedra rotate in a staggered fashion; i.e., neighboring octahedra rotate in opposite senses around parallel axes. With the choice of cubic axes given in Sec. II, the axis of rotation is parallel to [111] in the trigonal phase, to [101] in the orthorhombic phase, and to [001] in the tetragonal phase.

in having a ground state which is degenerate in cubic and trigonal symmetry. At low temperatures, when only the ground state is occupied, the Jahn-Teller effect by itself would favor a tetragonal distortion, since this gives the maximum splitting of the state. Competition between the two modes of distortion causes the axis of rotation itself to rotate, first to a $\langle 101 \rangle$ direction, giving the orthorhombic phase which is stable between 205 and 151 K; and finally to $\langle 001 \rangle$, giving the tetragonal structure observed below about 100 K.

While the 205-K transition is first order, so that the associated change in rotation axis is discontinuous, the 151-K transition is second order, and the axis moves continuously. It is the primary purpose of this investigation to study this continuous variation directly, using the electron spin resonance (ESR) of Gd^{3+} impurities as a probe. As we shall see, the Jahn-Teller interaction between Pr ions, being mediated by lattice strain, has a very long range and is not appreciably affected by the presence of the Gd impurity. ESR of impurities in crystals undergoing structural phase transitions has been used in several cases in the past, the most complete study being of Fe^{3+} ions in $SrTiO_3$ and $LaAlO_3$.[10] We have previously reported[8] some of the findings of the ESR studies of Gd^{3+} in $PrAlO_3$. In this paper we report the full results and analysis of this study. We give a fuller account of the experimental aspects in Sec. II. The analysis using conventional spin-Hamiltonian theory, by which the temperature dependence of the internal displacement order parameter is derived, is given in Sec. III.

An important objective of this work is to compare this order parameter, obtained by ESR, with the order parameters obtained from electronic split-tings and from macroscopic strain. While accurate measurements of the latter are available,[4] published optical data[3,6] are considerably less precise than our results. We therefore made optical-absorption measurements on the ground-state splittings, which are described in Sec. IV. Our results agree qualitatively with the fluorescence data of Harley et al.,[3] but are more precise. Furthermore, we could obtain the symmetries of the states from the polarization of the transitions, and thus confirm the assignments of Ref. 7 in the orthorhombic and tetragonal phases.

In Sec. V we compare the order parameters obtained from the three different types of measurements. Good agreement is obtained near T_c, but discrepancies appear in the region of the 118-K phase transition reported by Fleury et al.[12] Oddly enough, this transition has no detectable effect on the electronic splitting and macroscopic strain, and its effect on the internal displacement, though measurable, is quite small.

II. SPIN-RESONANCE MEASUREMENTS

A. Samples

All samples used in this study were flux grown and showed excellent {100}-type growth faces. (Here all crystallographic indices refer to the cubic-perovskite phase.) On the basis of preliminary measurements, we selected three samples which were single domain in the orthorhombic phase, and whose domain structure in the tetragonal phase could be switched by a magnetic field of 12 kG or less.[13] The latter property is an indication of low internal strain. Two samples were rectangular parallelopipeds containing nominally 1-at.% Gd^{3+}. substituted for Pr^{3+}. The third was a square platelet containing 0.03-at.% Gd^{3+}, as measured by spin resonance. Our results are independent of Gd content.

We use the following crystallographic conventions throughout the paper. The C_3 axis in the trigonal phase is labeled [111], the S_4 axis in the tetragonal phase [001]. Burbank[2] has shown that the true two-fold screw axis in the intermediate (orthorhombic) phase is at approximately 35° (rather than 90°) to [111], and we label this axis [101] (see Fig. 1). This screw axis is the rotation axis of the AlO_6 octahedra in this phase. The point symmetry at the Pr^{3+} site is C_{2v}, with the C_2 axis perpendicular to the screw axis, i.e., along [10$\bar{1}$]. This can be seen by inspection of Fig. 1 of Ref. 8.[14]

The actual distortion axes in a particular crystal depend on its state of strain. Our samples were very small, and were chosen for their lack of internal strain; consequently they were exceptionally sensitive to strain imposed from outside. The principal source of such strain is differential con-
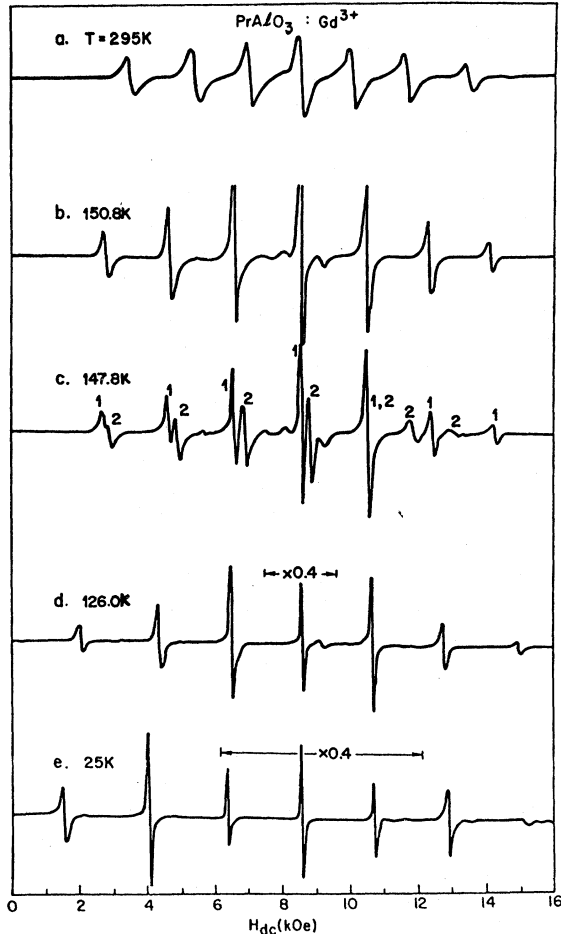
FIG. 2. Typical 24-GHz ESR spectra of Gd^{3+} in $PrAlO_3$ at different temperatures. (a) $\vec{H}_{dc} \parallel [111]$, trigonal phase; (b) $\vec{H}_{dc} \parallel [10\bar{1}]$, orthorhombic phase; (c) $\vec{H}_{dc}$ rotated by 9.5° from $[10\bar{1}]$ in the (010) plane, just below the 151-K phase transition (the lines marked 1 and 2 correspond to two domains as explained in the text); (d) same as (c), but well below the transition, with $\vec{H}_{dc}$ rotated by 27° from $[10\bar{1}]$ (the sample is now single domain); (e) $\vec{H}_{dc} \parallel [001]$, tetragonal phase. Note that the gain is reduced for the central lines in (d) and (e).

traction, especially if the sample is glued to some support. Changes in the mounting arrangements sometimes caused changes in the axes, and for consistent results the mounting had to be such as to minimize strain at all temperatures.

B. Spin-resonance measurements

Measurements were made in the absorption derivative mode at 24 and 34 GHz. At 24 GHz the sample was mounted on a polystyrene rod at the center of a cylindrical cavity, oriented to within 0.25° by x rays, and secured by a small quantity of silicone grease. With this method of mounting we found that the strain induced by differential contraction caused the 151-K transition to appear weak-

ly first order, instead of second order. For measurements very close to T_c we therefore placed the sample loosely in a slot in the mounting rod. It was then free of external strain and showed, as far as we could see, a good second-order transition. Because the sample could twist slightly in the magnetic field, this method of mounting led to an uncertainty of ± 1/2° in the orientation. Away from T_c the results obtained with both methods of mounting were the same. At 34 GHz a rectangular cavity was used, and the sample was oriented by placing the (010) face on the base of the cavity. We held it in place by gently packing with styrofoam. This arrangement gave a good second-order transition without introducing appreciable nonreproducibility in angle.

The cavity was cooled with flowing cold He gas and the temperature was stabilized to within 0.05 K with a heater fed back from a copper-constantan thermocouple thermally bonded to the outside of the cavity. In a separate experiment the temperature difference between the sample and the reference thermocouple was measured. The sample temperature was thus known absolutely to an accuracy of ± 0.5 K while the relative accuracy was ± 0.05 K.

Typical 24-GHz resonance spectra, taken with the direction of $\vec{H}_{dc}$ chosen to give the maximum separation between lines, are shown in Fig. 2. The spectra at 295 K were taken with $\vec{H}_{dc}$ rotating in the $(1\bar{1}0)$ plane and the spectrum shown is for $\vec{H}_{dc} \parallel [111]$. All other spectra shown in Fig. 2 were taken with $\vec{H}_{dc}$ rotating in the (010) plane. In Fig. 2(b) we note that the maximum splitting in the orthorhombic phase is obtained with $\vec{H}_{dc} \parallel [10\bar{1}]$; i.e., along the local C_2 axis, which is perpendicular to the C_3 axis of the trigonal phase (see Sec. II A).

In the b, c, and d spectra, weak lines due to the small twinned fraction of the crystal are observed near the $-\frac{1}{2} \rightarrow +\frac{1}{2}$ line (at ~8200 Oe). The linewidth varied with temperature, and with the orientation of the applied magnetic field. The sharpest line was the $-\frac{1}{2} \rightarrow +\frac{1}{2}$ transition (~30 Oe) at low temperatures while other lines were typically 50–200 Oe broad. This large linewidth (which may be connected with the finite magnetic susceptibility of the Pr^{3+} ion) almost obscured the slight broadening due to critical fluctuations near T_c, and excluded lineshape studies such as have been made, for instance, in the case of Fe^{3+} impurities in $SrTiO_3$. [10]

The domain structure which appears in the spectra below the 151-K phase transition plays an important role in the analysis. Figure 3 shows the angular variation of the spectra just above the orthorhombic-triclinic phase transition at 151 K and just below it. Below 151 K, when $\vec{H}_{dc}$ is rotated away from $[10\bar{1}]$ in the (010) plane each line splits into two lines designated 1 and 2 in Fig. 3(b).

a. 151K

+20°

+10°

[10Ī]

-10°

b. 149K

+20°

+10°

[10Ī]

-10°

0   4   8   12   16

H(kG)
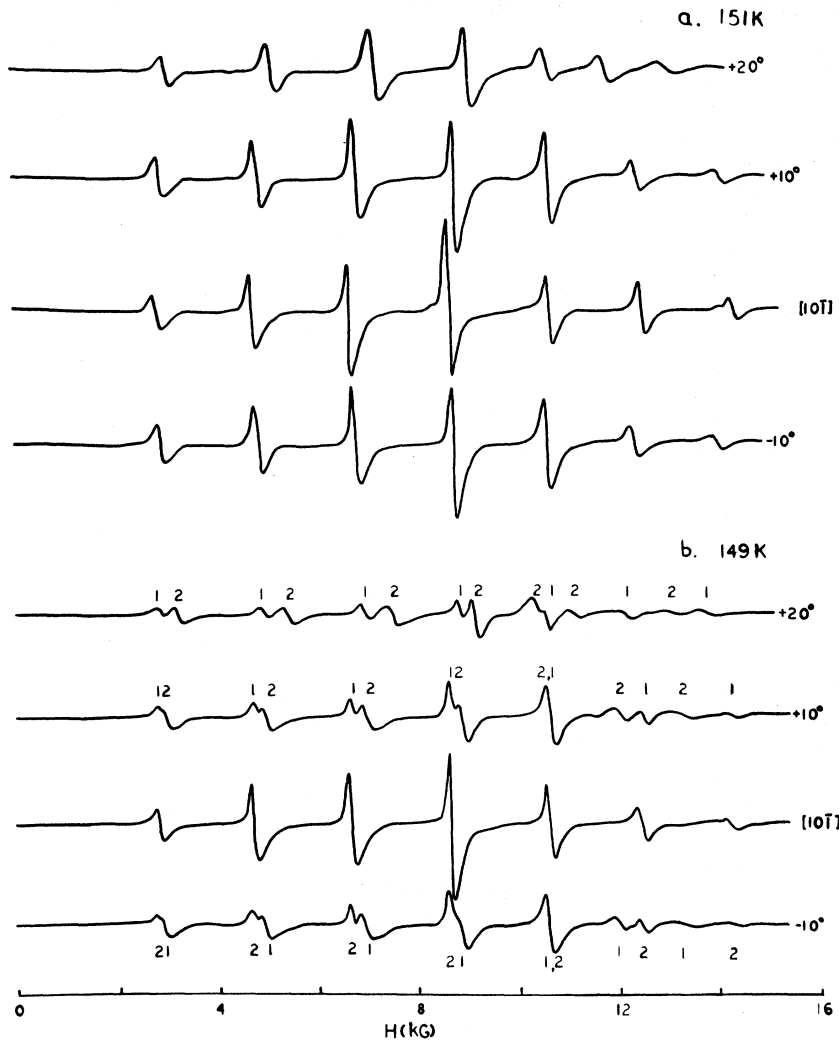
FIG. 3. Angular varia-
tion of the 24-GHz ESR
spectrum of Gd³⁺ in
PrAlO₃, just above and
just below the 151-K
transition, as $\vec{H}_{dc}$ is ro-
tated in the (010) plane.
The principal axes of the
spin Hamiltonian are found
from the angular varia-
tion of the two highest
field lines, as described
in the text.

Each set of lines corresponds to a domain with its
principal axis (direction for maximum separation
between resonance lines) rotated from the [10Ī]
axis towards either [001] or [100]. At about 125 K,
the domain with its axis rotating towards [100] usu-
ally disappeared and the crystal appeared to be
single domain down to low temperatures [Figs. 2(d)
and 2(e)].

Besides these measurements in the (010) plane,
we made some measurements on the same sample
in the (100) plane. We took care to preserve the
same domain structure as in the (010) measure-
ments. This was found to be impossible below
125 K. We found that, down to 125 K, the turning
point of the spectrum remains within 1° of [010].
This shows that one principal axis of the spin Ham-
iltonian remains parallel to [010], so that the other
two axes rotate in the (010) plane.

Precise 24-GHz measurements of the resonance
fields, for use in calculating the spin-Hamiltonian
parameters, were made at 295, 152, 123, and 25

K, with accuracy of between ±5 and ±20 G, accord-
ing to the linewidth.

In addition to the 24-GHz measurements a de-
tailed study of certain temperature regions was
made at about 34 GHz. We made careful search for
possible deviations from classical critical behavior
close to T_c. An advantage of working at the higher
frequency was that the field for resonance was then
high enough to make some of our samples single
domain, even close to T_c. This allowed us to make
measurements closer to T_c than in samples in
which the lines from two domains overlapped. A
further advantage was that the frequency of the
smaller cavity was found to be quite sensitive to
changes of sample dimensions and dielectric con-
stant. As a result we could locate the phase tran-
sition, even in zero magnetic field, through its ef-
fect on the dielectric constant and sample dimen-
sions, which is reflected in changes in the cavity
frequency. The frequency was measured to ±0.03
MHz (i.e., one part in 10⁶) with a Hewlett-Packard

transfer oscillator and frequency counter. The
precision with which the second-order transition
could be located was limited by its intrinsic width,
which in our best crystals was about 0.2 K. A
field of 18.5 kG was found to have no measurable
effect on the position or width of the transition.

Once it had been established by the 24-GHz mea-
surements that the most important effect of the
phase transition is the rotation of the principal
axes of the spin Hamiltonian in the (010) plane, it
was no longer necessary to make a complete angu-
lar diagram at every temperature. Instead, we
aligned $\vec{H}_{dc}$ at about 25° to $[10\bar{1}]$, in (010), and fol-
lowed the two highest resonances as a function of
temperature. The result of such a scan is shown
in Fig. 4, which covers a range from 1 above to
3 K below T_c in steps of about 0.2 K. The phase
transition shows up very clearly in such data. The
analysis of these data is not altogether straight-
forward, however, and will be dealt with in Sec.
III B.

III. ANALYSIS OF ESR DATA

In this section we show how our ESR data on Gd^{3+}
can be used to derive the direction of the rotation
axis of the AlO_6 octahedra, as a function of tem-
perature. We begin in A by defining the appropriate
spin Hamiltonian, and in B we show how we use our
data to find its principal axes. In C we develop a
phenomenological relation between the principal
axes and the rotation axis, and we give our results
in D.
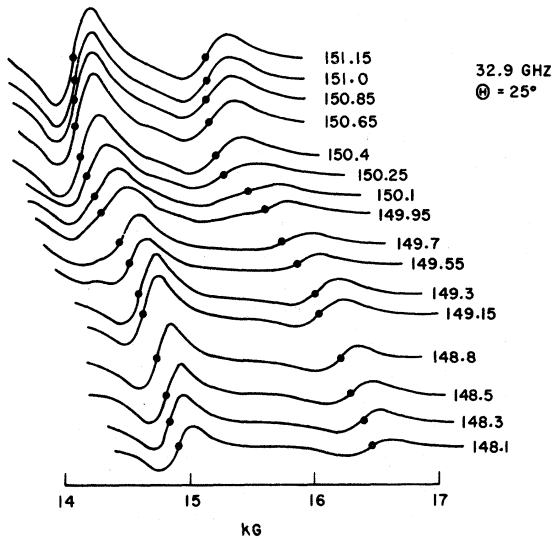
FIG. 4. 34-GHz ESR spectrum of a single domain
sample of $PrAlO_3$ containting about 1% Gd^{3+}. Tempera-
ture and absorption derivative are plotted vertically for
the two highest field transitions, with $\vec{H}_{dc}$ at 25° from
$[10\bar{1}]$. Temperatures shown have a relative accuracy
of ±0.05 K, and an absolute accuracy of ±0.5 K.
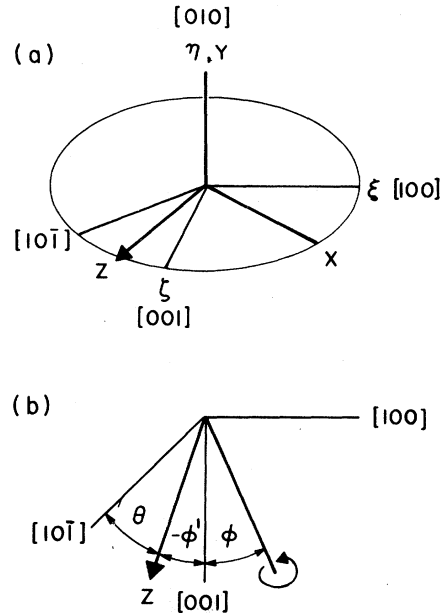
FIG. 5. (a) Coordinate systems for the cubic part of the
Hamiltonian (ξ, η, ζ) and for the axial part (x, y, z), in the
monoclinic phase. (b) Projection of (a) onto the (010)
plane, showing the axis of rotation of the AlO_6 octahedra
and the z axis of the spin Hamiltonian.

A. Spin Hamiltonian for Gd^{3+}

The spin Hamiltonian used to fit the observed
line positions has the form[15]

$$\mathcal{H} = g\mu_B \vec{H} \cdot \vec{S} + D[S_z^2 - \tfrac{1}{3}S(S+1)] + E(S_x^2 - S_y^2)$$
$$+ \tfrac{1}{6}a[S_\xi^4 + S_\eta^4 + S_\zeta^4 - \tfrac{1}{5}S(S+1)(3S^2 + 3S - 1)]$$
$$+ \tfrac{1}{180}F[35S_z^4 - 30S(S+1)S_z^2 + 25S_z^2 - 6S(S+1)$$
$$+ 3S^2(S+1)^2] , \tag{1}$$

with $S = \tfrac{7}{2}$. Here ξ, η, ζ refer to the cubic-perov-
skite axes, and do not change with temperature.
The deviation from local cubic symmetry is intro-
duced by the terms in x, y, z, axes which are tem-
perature dependent. The relation between the axes
is shown in Fig. 5(a). In the trigonal phase ($T > 205$
K) $\vec{z} \parallel [111]$ and in the orthorhombic phase ($151 < T$
< 105 K) the axes are selected as $\vec{z} \parallel [10\bar{1}]$, $\vec{x} \parallel [101]$,
and $\vec{y} \parallel [010]$. In the monoclinic phase ($T < 151$ K)
the z axis rotates from $[10\bar{1}]$ to $[001]$, almost reach-
ing the latter direction at low temperatures. The
parameters obtained by fitting the spin Hamiltonian
with 14 lines for each temperature are listed in
Table I. A sixth-order crystal-field term of cubic
symmetry was included in the fitting but its coef-
ficient found to be essentially zero. This result is
in accord with measurements on Gd^{3+} in other per-
ovskites.[16] The sign of D (and hence of all other
parameters) was determined by the relative intensi-
ties of the extreme lines at 4.2 K. The parameters

TABLE I. Spin-Hamiltonian parameters for Gd^{3+} in PrAlO$_3$.[a]

T (°K)	g	D	E	a	F
295	1.992 ±0.003	−0.0744 ±0.0003	0.0	−0.0015 ±0.0002	0.0002 ±0.0001
151	1.999 ±0.004	−0.0880 ±0.0005	−0.004 ±0.0005	−0.0002 ±0.0002	0.0002 ±0.0001
123	1.998 ±0.002	−0.0975 ±0.0003	−0.0014 ±0.0002	−0.0016 ±0.0002	0.0004 ±0.0001
25	1.999 ±0.003	−0.1039 ±0.0003	0.0	−0.0015 ±0.0002	0.0008 ±0.0002

[a]All parameters are in cm^{-1} (except for g). The sixth-order terms are zero within the accuracy of measurement.

given in Table I indicate that the fine structure of Gd^{3+} impurities in PrAlO$_3$ is mainly due to the second-order "D" term in the spin Hamiltonian. The fourth-order terms are small compared with the D term.

The only important fourth-order term is the cubic "a" term. It appears to be independent of temperature, except for an anomalously low value in the orthorhombic phase. This anomaly is probably an artifact of our fitting procedure, which is not well conditioned to distinguish between first-order effects of the a term and second-order effects of the "E" term. The value of a at other temperatures, about −0.0015 cm^{-1}, is in good agreement with data on Gd^{3+} in 12-fold oxygen coordination in other crystals.[16]

The second-order tensor is almost axial even in the monoclinic and orthorhombic phases, since $E/D \sim 0.01$ at 123 K and increases only to 0.05 at 151 K. The magnitude of D changes by 15% between 4.2 and 151 K.

B. Rotation of the principal axes as a function temperature

As described in Sec. II, the 24-GHz resonance spectrum for $125 \lesssim T < 151$ K consists of two sets of lines corresponding to two types of domains. We have measured the angular dependence of the ESR spectrum with $\vec{H}_{dc}$ in the (010) plane, as a function of temperature. The two highest field resonance lines are the most sensitive to angular variation. Their angular dependence is shown for a few typical temperatures in Fig. 6. It will be seen that for intermediate temperatures the curves for each domain are asymmetrical about their respective turning points (that is, about the position of maximum resonance field). Furthermore, the different transitions in the same domain have different turning points. This is because the cubic a term in the spin Hamiltonian produces an angle-dependent splitting which has turning points along [100]- and [110]-type directions, regardless of the axis of the D

term. We correct for this contribution to the splitting on the assumption that $a = -0.0015$ cm^{-1} at all temperatures. After this correction the curves are found to be symmetrical, with turning points that agree within the experimental accuracy of ±0.25°. The direction of $\vec{H}_{dc}$ at the corrected turning point is the z axis (principal axis) of the spin Hamiltonian of Eq. (1) for this domain. The z axes for the two domains are found to be rotated by equal and opposite amounts, which we denote $\pm \theta(T)$.

The limiting value of θ at low temperatures is found to be 44° ±0.5°, rather than 45°. It varies somewhat from sample to sample, and even from one domain to another in the same sample. This suggests that we can attribute the deviation from the ideal value of 45° to strain or impurity.

We now turn to the analysis of data obtained at fixed angle, such as that displayed in Fig. 4. The field for resonance is not a linear function of angle; furthermore, the spin-Hamiltonian parameters vary somewhat with temperature. Our procedure for obtaining the direction of the principal axis, as a function of temperature, is as follows. Let Θ be a general angle in (010), measured from [10$\bar{1}$]; let Θ_0 be the fixed angle at which the measurements were made and $\theta(T)$ be the direction of the principal axis. We made full rotation diagrams, as described above, at approximately 3-K intervals, thus obtaining $H(\Theta, T)$ and $\theta(T)$ at a few spot temperatures. Since $H(\Theta - \theta, T)$ depends only on D, E, and a, it is a slowly varying function of T, and can be accurately interpolated. Thus, comparison of the measured $H(\Theta_0, T)$, corrected for changes in cavity frequency, with the interpolated $H(\Theta - \theta, T)$ gives us $\theta(T)$ directly. The absolute accuracy of this procedure is only ±0.4°, but its precision is ±0.15°, and angles can be measured with a relative accuracy of this order.
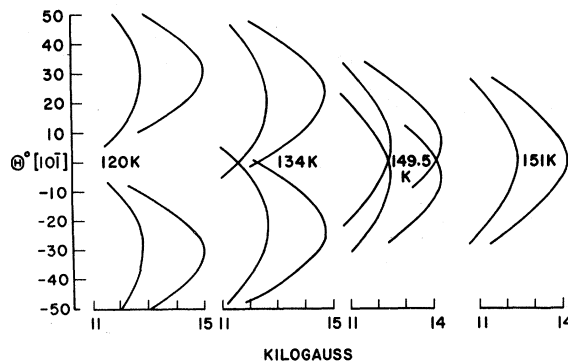
FIG. 6. Field for resonance at 24 GHz of the two highest field transitions of Gd^{3+} in PrAlO$_3$, plotted against angle Θ in the (010) plane, at some representative temperatures.

C. Derivation of the direction of local distortions

How are we to interpret $\theta(T)$, the angle by which the principal axes of the spin Hamiltonian are rotated in (010)? For an S-state ion like Gd^{3+}, the relationship between the local distortion, the crystal field, and the ground-state splitting is complex and not well understood.[17] In the orthorhombic and tetragonal phases, symmetry requires that the principal axes of the spin Hamiltonian coincide with the crystallographic axes, but there is no such requirement in the intermediate phase. However, we can show by a very general argument that there should be a definite and easily calculable relation between the principal axes of the D tensor and the axis of rotation of the AlO_6 octahedra.

We argue as follows. The D tensor (i.e., that part of the spin Hamiltonian which is quadratic in the spin operators) can be written in the general form

$$\mathcal{H}_s = \sum D_{\alpha\beta} S_\alpha S_\beta \ , \tag{2}$$

where α and β refer to the cubic axes ξ, η, and ζ. Because one axis is always [010], the local symmetry is at least C_s, and we have $D_{\xi\eta} = D_{\eta\zeta} = 0$. Our basic assumption is that all the other components of the D tensor can be expressed as smooth functions of a single temperature-dependent parameter, and that this parameter is an angle in the (010) plane. The only such angle in the model of Refs. 3 and 4 is the angle defining the axis of rotation of the AlO_6 octahedra. We call this angle ϕ, and measure it from [001]. We expand the components of the D tensor as a Fourier series in ϕ. Symmetry requires that the series have the form

$$D_{\alpha\alpha} = D_{\alpha\alpha}^{(0)} + D_{\alpha\alpha}^{(1)} \cos2\phi + D_{\alpha\alpha}^{(2)} \cos4\phi + \ldots \ ,$$
$$D_{\xi\zeta} = D_{\xi\zeta}^{(1)} \sin2\phi + \ldots \ , \tag{3}$$

where the coefficients are independent of temperature. We can determine these coefficients, though no higher ones, by considering only the limiting values of ϕ, which are 0, $\frac{1}{4}\pi$, and $\frac{1}{2}\pi$. For these we have the respective Hamiltonians

$$\mathcal{H}_s(0) = D[S_\zeta^2 - \tfrac{1}{3}S(S+1)] \ ,$$

$$\mathcal{H}_s(\tfrac{1}{4}\pi) = D'[S_z^2 - \tfrac{1}{3}S(S+1)] + E'(S_x^2 - S_y^2) \ ,$$

where

$$\vec{z} \| [10\bar{1}], \quad \vec{x} \| [101],$$

$$\mathcal{H}_s(\tfrac{1}{2}\pi) = D[S_\xi^2 - \tfrac{1}{3}S(S+1)] \ . \tag{4}$$

Here D is the observed spin-Hamiltonian parameter in the tetragonal phase and D' and E' the parameters in the orthorhombic phase.

Substituting Eqs. (2) and (3) in (4), and solving for the coefficients in (3), gives

$$D_{\zeta\zeta} + D_{\xi\xi} = -D_{\eta\eta} = [\tfrac{1}{2}E' + \tfrac{1}{6}(D+D')]$$
$$- [\tfrac{1}{2}E' - \tfrac{1}{6}(D - D')] \cos4\phi \ ,$$
$$D_{\zeta\zeta} - D_{\xi\xi} = D\cos2\phi \ , \tag{5}$$
$$D_{\xi\zeta} = -\tfrac{1}{2}(D' - E')\sin2\phi \ ,$$

plus higher terms which we cannot determine from the data available.

For general ϕ, the spin Hamiltonian (2) contains off-diagonal terms, but can be diagonalized by rotating the coordinate system through an angle ϕ'. In terms of the experimentally determined angle θ, measured from [10$\bar{1}$], we have $\phi' = \theta - \tfrac{1}{4}\pi$ [see Fig. 5(b)]. Then the relation between θ, ϕ, and ϕ' is found to be

$$\cot2\theta = -\tan2\phi' = \frac{-2D_{\xi\zeta}}{D_{\zeta\zeta} - D_{\xi\xi}} = \frac{D' - E'}{D}\tan2\phi \ . \tag{6}$$

The negative sign implies that ϕ and ϕ' have opposite signs. At T_c, $\phi = -\phi' = \tfrac{1}{4}\pi$; i.e., the rotation axis is perpendicular to the major axis of the spin Hamiltonian, as noted in Sec. II. For small θ, $(\tfrac{1}{4}\pi - \phi)/\theta = (D' - E')/D$. With our numbers, this ratio is 0.808 ± 0.008.

We can adduce two pieces of evidence supporting our basic assumption that the $D_{\alpha\beta}$'s are smooth functions of a single parameter. The first is the smallness of the $\cos4\phi$ term in (5); with our numbers its coefficient is about 1% of the terms in 2ϕ. The other is that Eq. (5) makes a definite prediction of the value of D and E for intermediate values of ϕ. For instance, at 123 K, where $\theta = 28°$, the predicted values are $D = -0.0973$, $E = -0.0016$ cm^{-1}. These agree with observation (see Table I) within experimental error. Of course, these facts only show that there is *some* angle ϕ in terms of which the D tensor can be expanded; the identification with the direction of the axis of rotation of the AlO_6 octahedra depends on the specific model.

Our result, Eq. (6), is identical in form to that obtained from the point-charge model (PCM), and used in our previous publication on this topic.[8] The PCM is, in fact, a special case of the general expansion used here; the PCM has the essential property that all calculated quantities are smooth functions of a single parameter ϕ. While the PCM is quite successful in describing the optical splittings of $PrAlO_3$ and $NdAlO_3$, it is known to have led to entirely wrong results for the high-order D splitting of the ground state of Gd^{3+}, whenever it has been applied.[17] The present calculation shows that the specific assumptions of the PCM can be dropped without affecting the relation between ϕ and θ.[18]

D. ESR results

We shall see in Sec. V. that $\cos2\phi$ is the appropriate order parameter to describe the internal displacements. The Landau theory of second-order
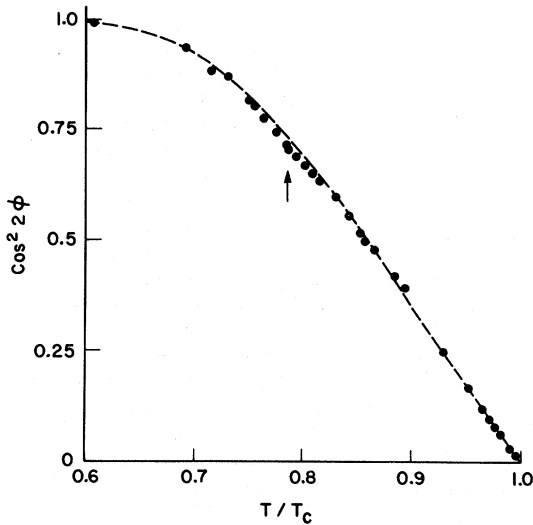
FIG. 7. Temperature dependence of $\cos^2 2\phi$, deduced from the ESR data. Below $0.6T_c$, $\cos^2 2\phi$ is essentially constant at 0.998 ± 0.002. The dashed line is a smooth curve through the data, ignoring the region around the 118-K transition (indicated by the arrow).

IV. OPTICAL MEASUREMENTS

We measured the optical absorption spectrum of PrAlO₃ in the region 20 000–20 800 cm⁻¹ on a Cary 14 spectrophotometer with a spectral slit width of 8–10 cm⁻¹. The transitions in this region all terminate on the $^3P_0$ excited state of Pr^{3+}, and originate on the lower crystal-field states of the $^3H_4$ ground level. The splitting of the lowest crystal-field doublet, whose temperature dependence is shown in Fig. 9, drives the cooperative Jahn-Teller phase transition. Both members of this doublet transform as A_1 in C_s (monoclinic) symmetry. There is also a low-lying state transforming as A_2, which remains at an almost constant energy from the ground state, and is not involved in the cooperative Jahn-Teller transition. We are concerned here (a) to establish the symmetry of the various states in the orthorhombic (C_{2v}) phase and (b) to measure more precisely the doublet splitting as a function of temperature.

A. Symmetries in the C_{2v} phase

Polarized absorption measurements were made on single-domain samples whose orthorhombic axes had been determined by ESR. We established in Sec. II that in a strain-free sample the z axis of the spin Hamiltonian [Eq. (1)] is the local C_2 axis [10$\bar{1}$], and is perpendicular to the rotation axis [101]. Having determined these direction in a crystal, we remounted it in a strain-free manner in the spectrophotometer. Typical polarized absorption spectra for the C_{2v} phase are shown in Fig. 10. The electric-dipole operators ex, ey, ez transform in C_{2v} as B_1, B_2, A_1 respectively.[19] The corresponding magnetic-dipole operators transform as B_2, B_1, A_2. Since the labeled transitions are electric dipole[20] and all terminate on the $^3P_0$ state, which

phase transitions predicts that the order parameter should vary as $(T_c - T)^{1/2}$ near T_c. In Fig. 7 we plot $\cos^2 2\phi$ against T/T_c over the entire range of temperature in which it has appreciable variation. Below $0.6T_c$ it has essentially reached its limiting value of 0.998 ± 0.002.

Figure 8 shows the region near T_c on an expanded scale. We see that the Landau relation is reasonably well obeyed for $0.9 < T/T_c < 0.995$. The slight deviation apparent near $0.985T_c$ is sample dependent and probably not significant. This "classical" behavior is expected when the effective interaction has a long range. The inelastic-neutron-scattering results[4] show that the range is indeed long, apparently of order 30 Å.

Another region of interest is the vicinity of 118 K, where Fleury has reported a pronounced acoustic anomaly.[12] Figure 7 shows that, away from 118 K, $\cos^2 2\phi(T)$ is convex upwards, but between 112 and 122 K there is a weak downwards convexity. This relatively small effect, corresponding to a displacement in θ of less than 1°, or alternatively a 10% change in slope of the $\cos 2\phi$-vs-T curve, is the only direct indication in our data of the 118-K transition.

We also looked for a change in cavity frequency in this region, such as might be produced by a dielectric anomaly or a dimensional change. Any deviation from a smooth dependence on temperature is less than one part in 2×10^5, for a filling factor of about 0.05. This is to be compared with the frequency shift of about 1 part in 10^4 observed in the first 1 K below the 151-K transition.

FIG. 8. Temperature dependence of $\cos^2 2\phi$ near the 151-K phase transition. The experimental transition temperature (marked T_c) is determined to ± 0.15 K by observing changes in the cavity frequency.
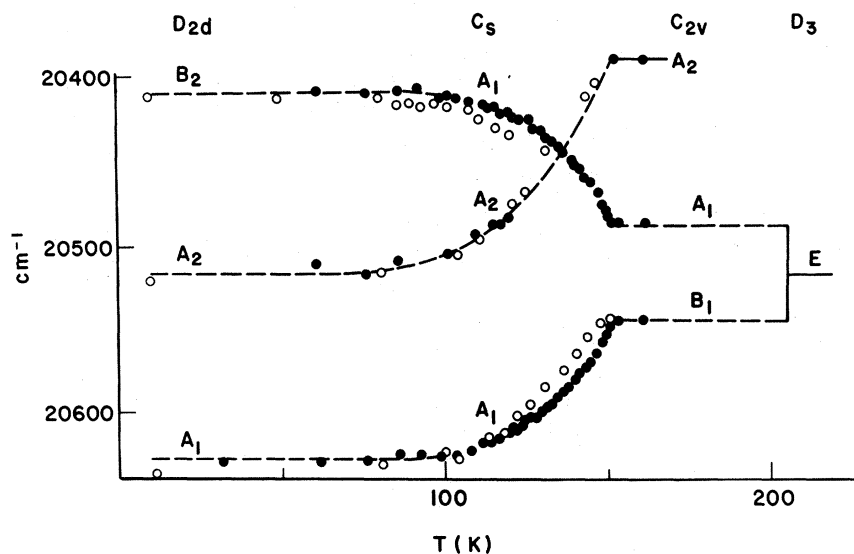
FIG. 9. Temperature dependence of the lowest crystal-field states of Pr^{3+} in $PrAlO_3$, relative to the $^3P_0$ excited state. Filled circles—absorption data of Sec. IV B; open circles—fluorescence data of Ref. 3. The symmetries of the states in the various phases are shown; these were determined from the polarization of the absorption lines in the C_{2v} and D_{2d} phases, and agree with the assignments of Ref. 7. The A_2 state cannot couple to the other two states shown, and plays essentially no role in the cooperative Jahn-Teller transition.

has A_1 symmetry in C_{2v}, the observed polarizations establish the symmetries shown. Table II shows the energies of the initial states of the transitions observed. The energies agree reasonably well with those found in fluorescence,[3] but we were unable to detect a transition from the second B_2 state, which according to Ref. 7 is around 310 cm^{-1}. Apart from this, the symmetries confirm the assignments made in the most recent crystal-field calculation,[7] which includes J mixing. They do not agree with previous assignments made on the basis of calculations which neglect J mixing.[4]

B. Temperature dependence of the ground-state splitting

The splitting between the lowest states (both A_1 in C_s symmetry) can be followed in absorption

TABLE II. Positions of the crystal-field states of the $^3H_4$ manifold of Pr^{3+} in the orthorhombic phase of $PrAlO_3$.

Absorption (cm^{-1})	Assignment	Fluorescence[a] (cm^{-1})	Calculated[b]	
0	B_1	0	0	B_1
59	A_1	57	36	A_1
155	A_2	160	171	A_2
253	A_1	238	240	A_1
255 ± 20[c]	B_2	282	271	B_2
...		...	322	A_2
...		311	306	B_2
357	B_1	357	361	B_1
...		821[d]	817	A_1

[a]Reference 3.
[b]Reference 7.
[c]Derived from a very broad transition.
[d]Raman data from Ref. 7.
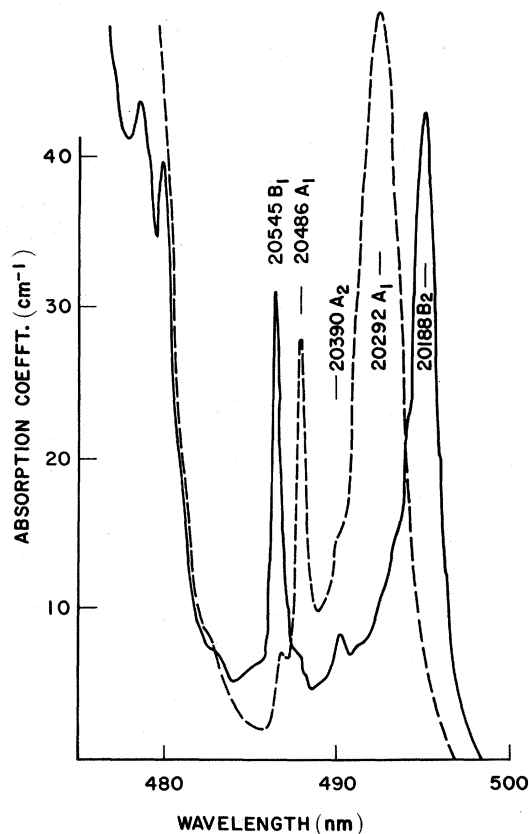
FIG. 10. Polarized absorption spectra of $PrAlO_3$ at 160 K. Dashed line—$\vec{E} \parallel [10\bar{1}]$ ($\bar{z}$); full line—$\vec{E} \parallel [101]$ ($\bar{x}$). Energies are given in cm^{-1}, and the labels are the symmetries of the initial states in C_{2v}. The spectrum for $\vec{E} \parallel [010]$ ($\bar{y}$) consists of a single very strong and broad line from a state or states of B_2 symmetry, centered near 20290 cm^{-1}.

down to about 60 K, where the excited state has too small a population to be visible in our 0.7-mm-thick sample. The results are shown as full circles in Fig. 9. The fluorescence data[3] are also shown: It will be seen that agreement is only qualitative, but could be improved by a change in temperature scale (T_c is given as 146 K in Ref. 3, which is 5 K below the accepted value). The discrepancy is not connected with the asymmetry of the lines. Even when this asymmetry is most severe, below 100 K, the difference between peak position and centroid is less than 5 cm⁻¹. Peak positions are used here, since they are easier to measure and probably give the best measure of the line position in unstrained portions of the crystal.

V. RELATIONS BETWEEN ORDER PARAMETERS

We have three different measures of order in this system: the angle ϕ, the macroscopic strain, and the splitting of the ground doublet. One can deduce an order parameter from each of these. According to the theory of cooperative Jahn-Teller phase transitions,[5] all three parameters should have the same temperature dependence near T_c.

In Ref. 4 a relation is derived between the macroscopic strain at temperature T, $(c-a)_T$, and the rotation angle ϕ:

$$(c-a)_T/(c-a)_0 = \cos 2\phi \quad . \tag{7}$$

This relation is based on a Hamiltonian containing lowest-order terms for the anharmonic interaction between the macroscopic strain and the local distortion coordinates, and follows directly from the assumption that the coupling is quadratic in these coordinates. It can also be obtained by simple geometry if we assume that the AlO_6 octahedra rotate as rigid units, and that the angle of rotation Ψ remains constant as ϕ varies. (The assumption of rigidity has been shown to hold in $SrTiO_3$.[21]) We find that Eq. (7) holds with $(c-a)_0/a_0 = \frac{1}{2}\Psi^2$, where a_0 is the cube edge. Taking $\Psi = 0.015$ (9°)[4] we find $(c-a)_0/a_0 = 0.012$, compared with the observed value of 0.014.[22]

In Ref. 4 it is also shown that if interaction with higher states is neglected, the splitting $W(T)$ of the ground doublet is related to the electronic order parameter $\langle \sigma_\zeta \rangle$ by

$$\langle \sigma_\zeta \rangle^2 = [W^2(T) - W^2(T_c)]/[W^2(0) - W^2(T_c)] \quad . \tag{8}$$

This is just the relation for an Ising system in a transverse field $W(T_c)$. If $W(T_c)$ were zero, the system would be identical with that studied theoretically by Feder and Pytte.[5] We can relate $\langle \sigma_\zeta \rangle$ to ϕ by a similar argument to that used for the D tensor. In order to do this we must assume that the crystal field is purely quadrupolar, so that it can be written in operator-equivalent form

$$V_{\text{cryst}} = \tfrac{3}{2}A_\eta[J_\eta^2 - \tfrac{1}{3}J(J+1)] + \tfrac{1}{2}(A_\zeta - A_\xi)(J_\zeta^2 - J_\xi^2) \quad , \tag{9}$$

with $J = 4$ and $A_\xi + A_\eta + A_\zeta = 0$. The apparently perverse choice of axes simplifies the algebra. Since we are only interested in the ground doublet, which transforms as E in O_h, terms like $J_\xi J_\eta$ are omitted from Eq. (9). We take as basis states $|3\eta^2 - r^2\rangle$, $|\xi^2 - \zeta^2\rangle$, and use the wave functions given by Griffith.[23] We find for the matrix form of the operator

$$V_{\text{cryst}} = \frac{4}{\sqrt{3}}\begin{pmatrix} \sqrt{3}A_\eta & A_\xi - A_\zeta \\ A_\xi - A_\zeta & -\sqrt{3}A_\eta \end{pmatrix} \quad . \tag{10}$$

The A's are functions of ϕ, analogous to the $D_{\alpha\alpha}$'s in Eq. (3). For $T = 0$, $\phi = 0$, we have

$$V_{\text{cryst}} = -\tfrac{3}{16}W(0)[J_\zeta^2 - \tfrac{1}{3}J(J+1)] \quad . \tag{11a}$$

For $T = T_c$, $\phi = \tfrac{1}{4}\pi$, and, in precise analogy with Eq. (4),

$$V_{\text{cryst}} = V_\theta[J_z^2 - \tfrac{1}{3}J(J+1)] + V_\epsilon(J_x^2 - J_y^2)$$
$$= -\tfrac{1}{2}(V_\theta + 3V_\epsilon)[J_\eta^2 - \tfrac{1}{3}J(J+1)] \quad . \tag{11b}$$

We do not need to know V_θ and V_ϵ independently, but only in the combination

$$W(T_c) = -\tfrac{8}{3}(V_\theta + 3V_\epsilon) \quad . \tag{12}$$

Here, positive $W(T_c)$ corresponds to the observed order of the levels in the orthorhombic phase.

We now assume, as in the case of the D parameters, that the A's are smooth functions of ϕ only. Since Eq. (11) is analogous to (4), we have, analogous to (5),

$$A_\eta = \tfrac{1}{32}\{[W(0) + 2W(T_c)] + [W(0) - 2W(T_c)]\cos 4\phi\} \quad ,$$
$$A_\xi - A_\zeta = \tfrac{3}{16}W(0)\cos 2\phi \quad . \tag{13}$$

For general ϕ the splitting is, from (10),

$$W(T) = \tfrac{8}{3}[A_\eta^2 + (A_\xi - A_\zeta)^2]^{1/2} \quad . \tag{14}$$

Whence

$$\langle \sigma_\zeta \rangle = \cos 2\phi \left(1 - \frac{q^2(1 - \cos^2 2\phi)}{(3+q)(1-q)}\right)^{1/2} \quad , \tag{15}$$

where $q = 2W(T_c)/W(0) - 1$.

For the observed value of q, about -0.45, the term in brackets lies between 0.97 and 1.0. Thus $\langle \sigma_\zeta \rangle$ should equal $\cos 2\phi$ within experimental error.

In Fig. 11 we compare the temperature dependence of the three order parameters, squared to illustrate the $(T_c - T)^{1/2}$ behavior near T_c. The full line is a smooth curve through the $\cos^2 2\phi$ values of Fig. 7. The crosses are the reduced macroscopic strain, $(c-a)_T^2/(c-a)_0^2$, obtained by elastic neutron scattering.[4] The circles are the values of $\langle \sigma_\zeta \rangle^2$ obtained by applying Eq. (8) to the data of Fig. 9. Down to $0.8T_c$ all three parameters agree with each other, and with the Landau $(T_c - T)^{1/2}$ law, within experimental error. Deviations begin in the
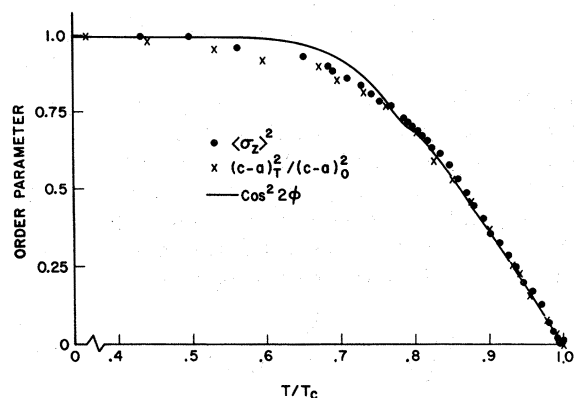
FIG. 11. Comparison of the three different order parameters associated with the 151-K phase transition. Full line—smooth curve through the data of Fig. 5 $(\cos^2 2\phi)$; circles— $\langle \sigma_\zeta \rangle^2$ derived from the data of Fig. 7, with the aid of Eq. (8); crosses— $(c-a)_T^2/(c-a)_0^2$ from the data of Ref. 4.

region of the 118-K transition. The weak anomaly in $\cos 2\phi$ is not reflected in the temperature dependence of $\langle \sigma_\zeta \rangle$, nor apparently in that of $(c-a)$, although this is less certain because of the wide spacing of the points. Below 118 K, $\cos 2\phi$ approaches its limiting value much more rapidly than the other two order parameters. It is not clear what connection, if any, this discrepancy has with the 118-K transition.

While agreement between $\langle \sigma_\zeta \rangle$ and $\cos 2\phi$ is excellent over much of the temperature range, it is somewhat surprising that this is so. The basic assumption leading to Eqs. (8) and (15) is that the ground doublet is isolated; interaction with higher electronic states is neglected. However, crystal-field calculations, both with[7] and without[4] J mixing, show that such interaction is not small. Thus, it is possible that the good agreement found here is fortuitous.

VI. SUMMARY

In this work we have measured the temperature dependence of two of the three order parameters describing the 151-K second-order transition of $PrAlO_3$. We find that all three agree for $0.8T_c < T < 0.995T_c$, and are proportional to $(T_c - T)^{1/2}$ over this range. This is the "classical" Landau behavior expected when the interaction is long range, as in this case. We find that simple semiphenomenological models describe the relation between the order parameters remarkably well. Our results agree with the more general theory of Feder and Pytte, even though their simple Ising model for the Jahn-Teller interaction is not strictly applicable to $PrAlO_3$ because of the presence of the "transverse" crystal field.

We find that the 118-K transition has only a small effect on the order parameters associated with the 151-K transition. This supports the view that the 118-K transition involves only macroscopic strain, this strain being orthogonal to the strain involved in the 151-K transition.

ACKNOWLEDGMENTS

*At Philips Research Laboratories, Eindhoven, 1973–1974, when part of this work was done.

†On leave of absence from the Department of Physics, Technion, Haifa, Israel.

[1]E. Cohen, L. A. Riseberg, W. A. Nordland, Jr., R. D. Burbank, R. C. Sherwood, and L. G. Van Uitert, Phys. Rev. 186, 476 (1969).

[2]R. D. Burbank, J. Appl. Cryst. 3, 112 (1970). Note that Burbank finds that the intermediate phases have lower symmetry than stated in the text: respectively, monoclinic and triclinic instead of orthorhombic and monoclinic. It is pointed out in Ref. 4 that the only evidence for this is one weak reflection, which may be spurious, which indicates a small displacement of the Pr^{3+} ions out of the symmetry plane. Such a displacement, if it exists, should have no appreciable effect on the interpretation of our data, and will be ignored.

[3]R. T. Harley, W. Hayes, A. M. Perry, and S. R. P. Smith, J. Phys. C 6, 2382 (1973).

[4]R. J. Birgeneau, J. K. Kjems, G. Shirane, and L. G. Van Uitert, Phys. Rev. B 10, 2512 (1974).

[5]J. Feder and E. Pytte, Phys. Rev. B 8, 3978 (1973).

[6]E. Finkman, E. Cohen, and L. G. Van Uitert, in Proceedings of the International Conference on Light Scattering in Solids, edited by M. Balkanski (Flammarion, Paris, 1971), p. 369.

[7]K. B. Lyons, R. J. Birgeneau, E. I. Blount, and L. G. Van Uitert, Phys. Rev. B 11, 891 (1975).

[8]E. Cohen, M. D. Sturge, R. J. Birgeneau, E. I. Blount, L. G. Van Uitert, and J. K. Kjems, Phys. Rev. Lett. 32, 232 (1974).

[9]K. A. Müller, in Proceedings of NATO Advanced Study Institute on Structural Phase Transitions and Soft Modes, Geilo, Norway, 1971, edited by J. Samuel-

son, E. Andersen, and J. Feder (Universitetsforlaget, Oslo, 1972), p. 61.

[10]Th. von Waldkirch, K. A. Müller, and W. Berlinger, Phys. Rev. B **5**, 4324 (1972); **7**, 1052 (1973).

[11]See papers accompanying Ref. 9.

[12]P. A. Fleury, P. D. Lazay, and L. G. Van Uitert, Phys. Rev. Lett. **33**, 492 (1974).

[13]L. A. Riseberg, E. Cohen, W. A. Nordland, Jr., and L. G. Van Uitert, Phys. Lett. A **30**, 4 (1969).

[14]We are grateful to E. I. Blount for drawing our attention to this important point.

[15]B. Bleaney and R. S. Trenam, Proc. R. Soc. Lond. A **223**, 1 (1954).

[16]R. L. White, G. F. Herrmann, J. W. Carson, and M. Mandel, Phys. Rev. **136**, A231 (1964); H. A. Buckmaster and Y. H. Shing, Phys. Status Solidi A **12**, 325 (1972).

[17]B. G. Wybourne, Phys. Rev. **148**, 317 (1966); H. A. Buckmaster, R. Chatterjee, and Y. H. Shing, Can. J. Phys. **50**, 78 (1972).

[18]This point is discussed in detail in the Appendix to Ref. 7. It is shown there that the form of Eq. (6) holds for any distribution of charges consistent with C_s symmetry, provided the deviation from cubic sym-

metry is small.

[19]G. F. Kôster, J. O. Dimmock, R. G. Wheeler, and H. Statz, *Properties of the 32 Point Groups* (MIT Press, Cambridge, Mass., 1963), p. 36. These authors' notation is related to ours as follows: $\Gamma_1 \rightarrow A_1$, $\Gamma_2 \rightarrow A_2$, $\Gamma_3 \rightarrow B_1$, $\Gamma_4 \rightarrow B_2$.

[20]The weak transition at 20390 cm^{-1} originates with the A_2 state at 155 cm^{-1}, and is electric-dipole forbidden. It appears to be predominantly magnetic dipole, but may have some electric-dipole character due to strain, or to the deviation from exact C_{2v} symmetry mentioned in Ref. 2.

[21]A. Okazaki and M. Kowaminami, in *Proceedings of the Third International Conference on Ferroelectricity, Edinburgh, Scotland*, 1973 (Gordon and Breach, London, 1974), p. 91.

[22]This assumption of rigidity must not be taken too seriously. It gives the wrong sign for the distortion of the trigonal phase of $PrAlO_3$ and $LaAlO_3$, and fails to account for the variation in length of the $\vec{b}$ axis in the monoclinic phase.

[23]J. S. Griffith, *The Theory of Transition Metal Ions* (Cambridge U. P., Cambridge, England, 1961), p. 393.